Journal of Marine Research, 42, 189–206, 1984

Variations in primary production and particulate carbon flux through the base of the euphotic zone at the site of the Sediment Trap Intercomparison Experiment (Panama Basin)

by James K. B. Bishop[1] and John Marra[1]

ABSTRACT

^{14}C primary production data collected during the deployment and recovery cruises of STIE in 1979 showed a simple relationship with light and nutrient concentrations in the euophotic zone. A simple empirical relationship, calibrated using these data, was derived so that weekly averaged observations of fractional cloudiness, sea-surface temperature and mixed layer depth could be used to estimate primary production on a weekly basis for the years 1976–1979. ^{15}N-uptake measurements, which estimate new production, were combined with the ^{14}C data to estimate particulate carbon fluxes from the euphotic zone.

Results of calculations showed that production may vary by a factor of three and particulate carbon flux by a factor of ten on a week to week basis with peak values corresponding to times when the mixed layer became enriched in nutrients. Mean euphotic zone production and particulate carbon flux estimated for the STIE deployment cruise were 286 and 138 mg C m^{-2} d^{-1}, respectively; they were 174 and 59 mg C m^{-2} d^{-1} for the recovery cruise. Mean production and flux values were 261 and 122 mg C m^{-2} d^{-1}, respectively for the duration of STIE. Three high production and particle sedimentation events may have occurred during STIE in September and October 1979. 1979 appeared to be a year of lower than average primary production compared with 1976 and 1977.

1. Introduction

The Sediment Trap Intercomparison Experiment (STIE) took place at 5N 82W in the Panama Basin between July and December 1979. During that time sediment traps of various designs were deployed on several moorings between depths of 600 and 3800 m to measure the vertical mass flux of particulate matter. Some moored traps had the ability to take sequential samples over time intervals of two and four weeks. Surface-tethered sediment traps were also deployed for 12 and 24 hour periods in the upper 300 m on both the trap deployment (*Knorr* 73-17) and recovery (*Gilliss* 7904/3) cruises. In addition, Large Volume *in situ* Filtration System (LVFS) profiles of particulate matter were obtained within the upper 1300 m over several day periods on both cruises. A major objective of STIE was to compare particle flux data derived from the collections of traps of different design and estimated indirectly from LVFS data.

1. Lamont Doherty Geological Observatory of Columbia University, Palisades, New York, 10964, U.S.A.

Table 1. Estimates of primary production in the Panama Bight*: mg C m^{-2} d^{-1}.

Location	January–April	May–December
Panama Bight Galathea Expedition May '52	—	370
Fixed Station 8°45'N, 79°23'W Nov '54–June '59	750	370
Panama Bight ACENTO May '65–Feb '67	550–650	100–290
Panama Bight EASTROPAC 77 Jan–Feb '68	900	—

*From Forsbergh (1969, Table 28).

The Composition Flux and Transfer Experiments (C-FATE[2]) occurred on the same cruises as STIE and were designed to complement STIE by providing a biological and suspended particulate matter data set which would augment our understanding of the linkage among the physical environment, biological processes, and particle sedimentation. Since the particle flux in the Panama Basin at 1N, 86W may vary substantially over weekly to seasonal time scales (Bishop *et al.*, 1980), an additional goal of C-FATE was to provide a basis for comparison of particle flux measurements made during different periods of time during STIE.

Few primary production data exist for the STIE area. This area, however, lies west of the Panama Bight (defined as the eastern equatorial Pacific between 1 and 9N and east of 81W) where Forsbergh (1969) has provided a summary of the climatology, oceanography, and fisheries. Hydrographic data collected within the Bight, indicate that upwelling activity and shallow mixed layer occur from January to March, after which the mixed layer deepens through the rest of the year. Chlorophyll *a* and primary production (Table 1) in the Bight respond to the upwelling, so that peak values, occurring in March, may be double the annual average values. Zooplankton populations, lagging the phytoplankton, double by March and increase a further 50% by May to June. Abundances fall off gradually through November. Fish harvest generally follows that of zooplankton abundance. We assume that the STIE area, by its proximity, will be influenced, but at a reduced level, by the major upwelling events in the Panama Bight as described by Forsbergh.

In this paper, we intend to extend Forsbergh's work and provide a history of the variability of primary production at 5N, 82W from 1976–1979 and, we hope, a better understanding of one of the major factors governing the vertical flux of particulate

2. (P. E. Biscaye, J. K. B. Bishop, W. D. Gardner, J. Marra, A Bé at L-DGO and P. Wiebe W.H.O.I)

matter into sediment traps during STIE. Toward this end, rather than constructing a complicated primary production model such as, for example, described in Platt *et al.* (1977), we formulate a simple empirical relationship, calibrated against C-FATE data, to predict primary production as a function of photosynthetically active radiation (*PAR*), seasurface temperature (*SST*), and depth of the mixed layer (*DML*). As we shall show, the latter two variables provide indications of the nutrient content of the euphotic zone. Since weekly averages of cloudiness (*C*), *SST* and *DML* are available for the STIE area from NOAA/NMFS (La Jolla) the relationship can be used to estimate production during the periods for which ship data are not available. In the discussion below, we draw on the concepts of "new" (upwelled or entrained) and "regenerated" (recycled) nutrients supporting production (Dugdale and Goering, 1967) and of new production being equal to particulate carbon flux through the base of the euphotic zone (Eppley and Peterson, 1979).

2. Derivation of the empirical primary production relationship

Primary production (*PP*) occurs as a direct consequence of the availability of sunlight and of nutrient supply. While solar radiation attenuates with depth, nutrients are supplied from the deep by processes of upwelling or turbulent entrainment of the mixed layer. As the processes that supply nutrients to the mixed layer also tend to reduce *SST*, we shall derive, in this section, a relationship between *PP* and *PAR*, *SST* and *DML* which were available or estimable from ship board measurements during C-FATE.

The water in the euphotic zone of the STIE area is divisible into two major layers. The upper layer, or the mixed layer, represents a nutrient-limited regime (except when enriched by nutrients due to entrainment and/or upwelling) while the lower layer, or the upper thermocline, represents a region where production is limited by light rather than by nutrients. During STIE, the mixed layer had typical properties of 27°C, 32 parts per thousand salinity (‰ S), and 0.04, 0.02, <.1, 0.19, and 1.5 μmol kg^{-1} of nitrate (NO_3), nitrite (NO_2), ammonia (NH_3), phosphate (PO_4), and silicate (Si), respectively. The lower layer was characterized by marked gradients in which 15°C, 35‰ S, and 27, 2.0 and 18 μmol kg^{-1} values of NO_3, PO_4, and Si were reached by 70 m. Maxima in NO_2 and NH_3 of 0.7 and 0.3 μmol kg^{-1} were found several meters below the base of the mixed layer and decreased to undetectable levels by 70 m (Bishop and Spencer, unpublished data). The deepest limit of the second layer (70 m) was chosen because it corresponded approximately to the depth of 1% of *PAR* at the surface and thereby defines the lower limit of the euphotic zone. This distribution of environmental variables resulted in a subsurface maximum in production a few meters below the base of the mixed layer (Marra *et al.*, 1983).

PP values at various depths come from the dark bottle-corrected ^{14}C measurements described by Marra *et al.* (1983). The total ^{14}C production in the euphotic zone is

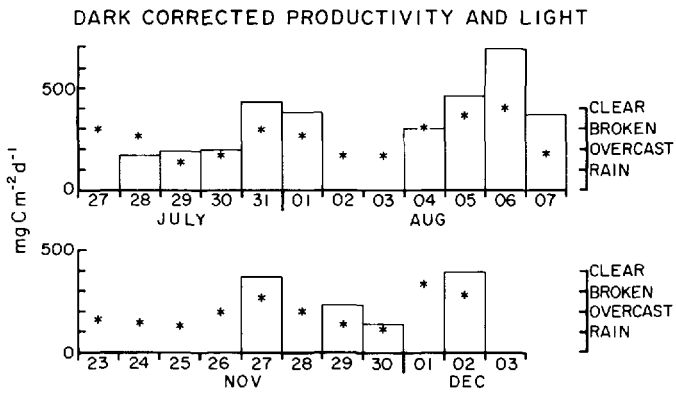

Figure 1. Integrated primary production in the euphotic zone for both *Knorr* and *Gilliss* cruises (bars) compared with mean day-time cloudiness data obtained from ship's logs (*).

plotted together with estimates of cloudiness (Fig. 1) and demonstrates the importance of light availability as a controlling factor of *PP*.

The *PP* in the second layer attenuates with depth, as to be expected from its dependence on *PAR*. In order to estimate *PAR* as a function of depth we assume:

1) The relationship between cloud cover (C) and solar radiation incident at the sea surface, I_i, is described by that given in Johnson *et al.* (1965),

$$I_i = I_s(1 - 0.4*C - 0.38*C^2) \tag{1}$$

where I_s is solar radiation on a cloud-free day. This is one of several quantitative relationships that are commonly used. Monthly average I_s values at 5N 82W range between 590 (Dec) and 670 Ly d^{-1} (Mar, Apr, and Sept) with a mean of 645 Ly d^{-1} (Ivanoff, 1977) and are listed in Table 2. Values were 650 and 605 Ly d^{-1} (1 Ly d^{-1} = 0.484 Watts m^{-2}) for the *Knorr* and *Gilliss* cruises respectively.

2) Photosynthetically active radiation (*PAR*), or the blue-green portion of solar radiation absorbed at the sea surface, I_o, is given by Strickland (1958),

$$I_o = 0.5* I_i \tag{2}$$

3) *PAR* decreases exponentially with depth (Ivanoff, 1977) so that *PAR* at some depth z, I_z, is related to its surface value by:

$$I_z = I_o e^{-kz} \tag{3}$$

where k is the mean extinction coefficient for light. To estimate k, Secchi disk measurements were made on the *Knorr* and *Gilliss* cruises. Secchi depths obtained were 24.7 ± 2.0 m and 22.0 ± 2.3 m (σ) respectively giving a mean of 23.5 m. Assuming that three times the secchi depth (or 70 m) is equal to the 1% light level (Eppley *et al.*, 1979), k is computed to be 0.066 m^{-1} for the euphotic zone.

Table 2. Primary production and particle flux estimates for 1979 (T_{crit} = 26.5).

Day	*SST*	*DML*	I_s	*C*	*TPP*	$xsPP_{ml}$	*FLUX*	*xsFLUX*	*FLUX/TPP*
				Model results based on NOAA data					
7	26.5	30.4	610	0.59	200.5		78.4		0.391
14	27.0	15.2	610	0.59	308.9		153.9		0.498
21	25.7	14.0	610	0.59	550.4	966.0	302.7	531.3	0.550
28	27.0	22.9	610	0.59	238.9		107.4		0.449
35	25.0	22.9	650	0.48	609.7	2394.9	335.4	1317.2	0.550
42	29.0	15.2	650	0.48	351.6		177.4		0.505
49	28.0	15.2	650	0.48	351.6		177.4		0.505
56	28.0	15.2	650	0.48	351.6		177.4		0.505
62	27.0	22.9	670	0.48	272.2		125.7		0.462
69	27.0	14.6	670	0.48	367.2		186.6		0.508
76	26.5	15.2	670	0.48	358.8		181.4		0.506
83	27.0	14.3	670	0.48	371.5		189.3		0.510
98	26.5	14.6	670	0.63	324.0		162.9		0.503
106	27.5	15.2	670	0.63	316.7		158.2		0.500
113	28.2	15.2	670	0.63	316.7		158.2		0.500
120	28.5	15.2	670	0.63	316.7		158.2		0.500
128	29.0	38.1	650	0.75	173.5		55.4		0.319
135	27.8	38.1	650	0.75	173.5		55.4		0.319
142	28.5	36.5	650	0.75	174.8		57.8		0.331
149	28.7	33.5	650	0.75	178.7		63.1		0.353
154	27.5	47.0	640	0.80	168.5		44.5		0.264
161	28.0	38.0	640	0.50	191.1		65.2		0.341
168	27.8	31.0	640	0.70	189.2		71.5		0.378
175	26.7	23.0	640	0.80	200.8		86.3		0.430
181	26.2	14.0	640	0.65	538.6	626.4	296.3	344.5	0.550
188	26.6	30.0	640	0.85	170.4		62.2		0.365
196	27.5	32.0	640	0.80	174.3		62.2		0.357
203	27.0	25.0	640	0.80	192.5		79.6		0.414
*209	27.9	18.0	640	0.60	285.5		138.1		0.484
*217	27.5	29.0	660	0.60	212.1		86.2		0.406
225	27.5	12.0	660	0.85	263.3		132.2		0.502
230	27.5	30.0	660	0.88	167.3		60.5		0.362
237	27.0	30.0	660	0.75	187.4		71.6		0.382
244	26.5	38.0	670	0.88	163.1		49.8		0.305
251	26.0	38.0	670	0.75	499.0	2355.6	274.5	1295.6	0.550
259	25.5	31.0	670	0.85	428.8	2688.4	235.8	1478.6	0.550
266	26.6	24.0	670	0.80	200.9		85.3		0.425
273	26.3	24.0	670	0.70	527.6	1034.6	290.2	569.0	0.550
280	26.5	27.0	660	0.80	188.1		75.1		0.399
287	26.5	26.0	660	0.75	201.2		83.4		0.414
294	27.1	32.0	660	0.85	169.2		59.5		0.351
301	26.2	28.0	660	0.80	461.7	1423.5	253.9	782.9	0.550
308	26.8	21.0	620	0.70	231.5		105.3		0.455

Table 2. (Continued)

Day	*SST*	*DML*	I_s	*C*	*TPP*	$xsPP_{ml}$	*FLUX*	*xsFLUX*	*FLUX/TPP*
Model results based on NOAA data									
315	26.5	32.0	620	0.85	166.1		57.7		0.348
322	27.0	28.0	620	0.75	188.5		74.3		0.394
*329	27.8	26.0	620	0.75	195.4		80.2		0.410
*336	26.5	18.0	590	0.80	218.4		101.2		0.463
343	27.5	21.0	590	0.60	246.0		113.3		0.460
Model results based on mean of C-FATE observations of *SST*, *DML* and *C*									
213	27.0	18.0	640	0.60	285.5		138.1		0.484
333	27.0	35.0	620	0.75	174.1		59.0		0.339

day – Julian day

*—weeks where C-FATE data collected at sea.

Eqs. 1 to 3 allow us to estimate I_z, the *PAR* at some depth z as a function of cloudiness C. Exact values of C are traditionally difficult to ascertain. We have assigned $C = 0, 0.50, 0.75$ and 1.00 on days having clear, broken cloud, overcast, and overcast with rain conditions respectively. Mean daily fractional C values were calculated by averaging ship's log entries made at three times per daylight period and interpolating to the above scale.

Figure 2 shows C-FATE *PP* data from depths below the mixed layer plotted against I_z. We assume that the response of primary production to *PAR* in the absence of nutrient limitation can be approximated by a parabolic fit to these data. The correlation coefficient for this fit to the data averaged over 5 Ly d^{-1} intervals (large symbols, Fig. 2) was 0.87. It must be noted that a linear fit to the data (correlation coefficient 0.86) is equally satisfactory statistically. The parabolic fit would predict rising production to a maximum of 21 mg C m^{-3} d^{-1} as I_z increases to 164 Ly d^{-1} and then a drop off in production at higher light levels. We assume that production is constant at 21 mg C m^{-3} d^{-1} for $I_z > 164$ Ly d^{-1}. This threshold light value for maximal photosynthetic production in the absence of nutrient limitation is consistent with that found, for example, by Yentsch and Lee (1966), Dunstan (1973) and Kiefer (1973). Therefore, we adopt the parabolic fit to the data with the addition of the above constraint in favor of the linear fit,

$$\begin{aligned} PP_{\text{L.lim.}} &= a + bI_z + cI_z^2, I_z < 164 \text{ Ly d}^{-1} \text{ mg C m}^{-3} \text{ d}^{-1} \\ &= 21, I_z \geq 164 \text{ Ly d}^{-1} \end{aligned} \tag{4}$$

where $a = 0.536$, $b = 0.252$, and $c = -0.00077$. Although this formulation is not typical of that found in primary production models based on irradiance (eg. Jassby and Platt, 1976), it approximates the response of *PP* to I_z adequately.

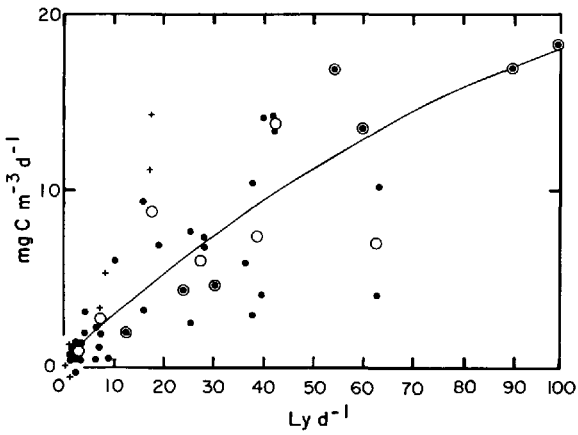

Figure 2. Parabolic fit of primary production for samples below the mixed layer against calculated *in situ* photosynthetically active radiation. *Knorr* 73-17 and *Gilliss* 7904/3 data are indicated by (•) and (+), respectively. Averaged values used in the fit are indicated by (O).

The mean mixed layer production values for the *Knorr* and *Gilliss* cruises were 3.3 and 2.8 mg C m^{-2} d^{-1}, respectively. Since the mixed layers during these cruises had *SST* values of 27°C and were depleted of nutrients, it is assumed that the mean value of 3.0 mg C m^{-3} d^{-1} is typical of nutrient-limited production in the model. The co-occurrence of warm *SST* and low nutrient levels is the key to using *SST* data (see below) as an indication of nutrient depleted conditions in mixed layer.

$$PP_{\text{N.lim.}} = 3.0 \text{ mg C m}^{-3} \text{ d}^{-1} \tag{5}$$

Profiles of production for a 20 m nutrient-limited layer overlying a 50 m thick light-limited layer calculated using Eqs. 4 and 5 and C values of 0. (brightest day), 0.6 (average cloudiness for the *Knorr* cruise) and 1.0 show reasonable agreement with the *Knorr* data (Fig. 3). *Gilliss* data show higher values than predicted by similar calculations for a 35 m nutrient-limited layer overlying a 35 m thick light-limited layer but this may be attributed to the fact that the *Gilliss* data were less systematically collected than the *Knorr* data.

a. Euphotic zone production estimates. In the nutrient limited case, the integrated production over a depth interval ($Z_1 < Z < Z_2$) is,

$$\Sigma PP_{\text{N.lim.}} = \int_{Z_1}^{Z_2} PP_{\text{N.lim.}} dz \text{ mg C m}^{-2} \text{ d}^{-1} = 3.0(Z_2 - Z_1) \tag{6}$$

In the light-limited case, the integrated production over a depth interval ($Z_1 < Z < Z_2$)

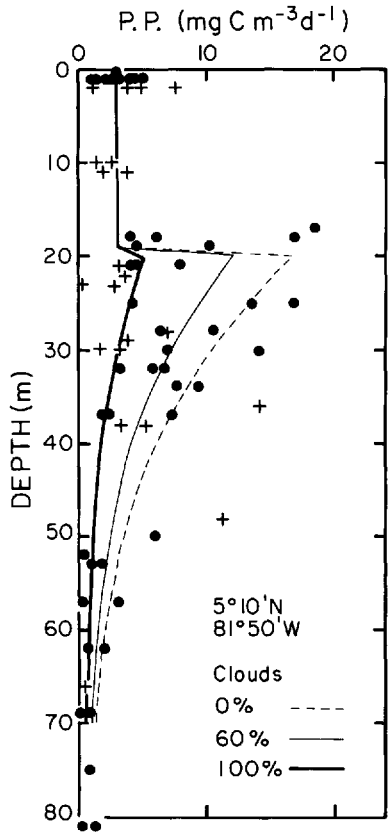

Figure 3. Computed fit (assuming various values for cloudiness and a mixed layer depth of 20 m and nutrient limiting conditions in the mixed layer) compared with dark corrected productivity data measured on both *Knorr* and *Gilliss* cruises. The *Gilliss* data are considered less reliable than the *Knorr* data.

is calculated from Eq. 4,

$$\begin{aligned}\Sigma PP_{\text{L.lim}} &= \int_{Z_1}^{Z_2} PP_{\text{L.lim}}\,dz \quad \text{mg C m}^{-2}\text{d}^{-1} \\ &= PP_{\max}(Z_{**} - Z_1) + a(Z_2 - Z_{**}) - bI_o/k[e^{(-kZ_2)} - e^{(-kZ_{**})}] \\ &\quad - cI_o^2/2k[e^{(-2kZ_2)} - e^{(-2kZ_{**})}] \end{aligned} \tag{7}$$

where $PP_{\max} = 21$ mg C m^{-3} d^{-1} at the depth, Z_{**}, where $I_z = 164$ Ly d^{-1}. If $Z_{**} < Z_1$ then it is set equal to Z_1.

Estimates of mixed layer production may be made using Eqs. 6 and/or 7. On a cloudy day production in a very deep mixed layer may be limited by light as well as by nutrients, whereby the 3 mg C m^{-3} d^{-1} production assumed in the nutrient-limited case exceeds the value computed assuming only light limitation. In this case the production

profile is determined by the lower of the two values. Thus, integrated mixed layer production, ΣPP_{ml}, in the nutrient limited case is given by:

$$\Sigma PP_{ml} = \int_0^{Z_*} PP_{\text{N.lim.}} dz + \int_{Z_*}^{Z_{ml}} PP_{\text{L.lim}}\, dz \text{ mg C m}^{-2} \text{ d}^{-1} \tag{8}$$

where Z_* is the depth where light-limited production equals 3.0 mg C m^{-3} d^{-1} and Z_{ml} is the mixed layer depth. If Z_* is calculated to be deeper than the mixed layer depth then Eq.(8) reduces to Eq. (6) with $Z_1 = 0$ and $Z_2 = Z_{ml}$.

From time to time, there have been reports of high production in the mixed layer (Forsbergh, 1969, Love *et al.*, 1970–1977). Hydrographic data show that these events are accompanied by lower sea-surface temperatures and higher salinities and nutrient concentrations. These events are probably caused by upwelling or by mixing of deeper water into the mixed layer. C-FATE hydrographic data show an inverse linear relationship between nutrient concentration and temperature over a temperature range of 7°C to 27°C (Fig. 4). We therefore expect that any relative drop in SST due to entrainment from below the mixed layer will be accompanied by a proportional increase in nutrients. We will use this knowledge to develop criteria for predicting high production in the mixed layer based on SST data.

We start by assuming that there exists a critical temperature, T_{crit}, such that production is nutrient-limited for all $SST \geq T_{\text{crit}}$ and that production is light-limited for $SST < T_{\text{crit}}$:

$$\Sigma PP_{ml} \begin{cases} = \int PP_{\text{N.lim.}} dz, & SST > T_{\text{crit}} \\ = \int PP_{\text{L.lim.}} dz, & SST < T_{\text{crit}} \end{cases} \tag{9}$$

We have chosen T_{crit} to be 26.0°C for several reasons. Firstly, there is sufficient nutrient content in a mixed layer colder than 26°C to support high production for one week. Figure 4 shows that an inverse linear relationship exists between PO_4 and T for samples collected during both STIE cruises. PO_4 is generally not considered to limit production at the concentration levels found in the 27°C mixed layer. The NO_3 levels are low enough, however, to limit production. Unfortunately, NO_3 data were collected only on the *Knorr* cruise and were not generally accompanied by temperature measurements. PO_4 analyses on some of the same water samples measured for NO_3 did indicate a linear relationship between PO_4 and NO_3 (Bishop and Spencer, unpublished data). Thus we assume that temperature can be used as an indicator of NO_3 as it can be for PO_4. We calculate that NO_3 increases from 0.04 μmol at 27°C to 27 μmol at 15°C at a rate of 2.3 μmol $°C^{-1}$. Thus a one degree drop in SST from 27°C to 26°C is accompanied by an increase in NO_3 from 0.04 to 2.3 μmol kg^{-1}. Assuming that the produced organic matter has a C/N ratio of 7 and that all organic matter is quantitatively removed from the mixed layer, then this increase of NO_3 is sufficient to sustain maximum production at 21 mg C m^{-3} d^{-1} for 9 days and thus guarantees an unlimited supply of nutrients for the one week period used in the calculation. A second

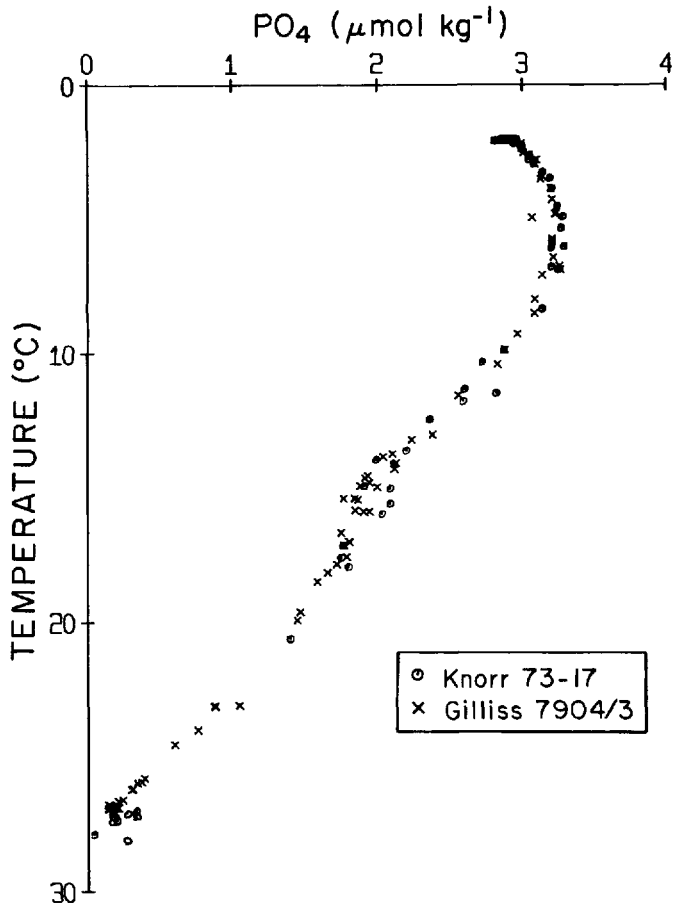

Figure 4. Phosphate—Temperature plot for both *Knorr* and *Gilliss* cruises.

reason for choosing $T_{crit} = 26.0°C$ is that there is some error involved in the production of the NOAA maps and in interpolating SST data from them. A final reason is that we are interested only in major entrainment and upwelling events, not those which support mixed layer production at other times.

Integrated production below the mixed layer is given by Eq. 7 since there is always high nutrient availability in this zone,

$$\Sigma PP_{bml} = \int_{Z_{ml}}^{Z_{eu}} PP_{\text{L.lim.}}\, dz \tag{10}$$

where $Z_{eu} = 70$ m is the euphotic zone depth. Total euphotic zone production is the sum of integrated production values for the mixed layer and below the mixed layer.

$$TPP = \Sigma PP_{ml} + \Sigma PP_{bml} \tag{11}$$

b. Euphotic zone particulate carbon flux estimates. Eppley and Peterson (1979) assumed that particulate flux from the euphotic zone is equal to new production. New production estimates were made on the *Knorr* cruise only and data provided to us by R. Eppley showed that new production averaged 20% of the ^{14}C production in the nutrient-limited mixed layer and 55% of the ^{14}C production below the mixed layer. We assume that these ratios are applicable in general to nutrient-limited and light-limited conditions. Hence particulate carbon flux from the mixed layer and below the mixed layer is given by,

$$FLUX_{ml} \begin{cases} = \Sigma PP_{ml}*0.2, SST \geq T_{\text{crit}} \\ = \Sigma PP_{ml}*0.55, SST < T_{\text{crit}} \end{cases} \tag{12}$$

$$FLUX_{bml} = \Sigma PP_{bml}*0.55 \tag{13}$$

Total particulate carbon flux is calculated by summing Eqs. 12 and 13.

$$T.FLUX = FLUX_{ml} + FLUX_{bml} \tag{14}$$

Before examining model results, several caveats must be made. First, production in the model has no explicit dependence on phytoplankton biomass. This is supported by evidence that zooplankton grazing maintains phytoplankton biomass at a constant level over time periods less than a week (Marra *et al.*, 1983). The high stratification of the euphotic zone coupled with the relatively rare cases of high mixed layer production (see below) would tend to stabilize the phytoplankton—zooplankton relationship. Another major assumption is that each week is decoupled from the next. A consequence of decoupling is that there may be excess nutrients left in the mixed layer after an entrainment event and a week of high mixed layer production. This excess is ignored in our simple formulation but we can estimate the particulate carbon flux necessary to completely deplete the mixed layer of nutrients. This excess flux is given by,

$$xsFLUX = ((T_{\text{crit}} + 1) - SST)*2.3*7*12*Z_{ml} - FLUX_{ml}, \tag{15}$$

where T_{crit} is the transition temperature for light-limited production, 2.3 is rate of increase of NO_3 with decreasing temperature, 7 is the assumed C/N mole ratio of the produced organic matter and 12 is the atomic weight of carbon. This when summed with new production estimated above provides an upper constraint on weekly averaged particulate carbon flux from the mixed layer. By applying the 55% ratio of particulate carbon flux to total production under light limitation we can estimate the excess production for the mixed layer,

$$xs\Sigma PP_{ml} = xsFLUX/0.55 \tag{16}$$

There are several ways to deal with the $xsFLUX$ and $xs\Sigma PP_{ml}$ unaccounted for by the model. The first would be to assume that the ^{14}C and ^{15}N data were both biased low by

Table 3. Seasonal and yearly mean production and particle flux estimates.

				yearly averages				seasonal averages January–April				May–August				September–December			
				P. Prod.		V. Flux		P. Prod.		V. Flux		P. Prod.		V. Flux		P. Prod.		V. Flux	
T_{crit}	Year	#obs.	%Hi.	mean	lim.	mean	lim.	mean	lim.	mean	lim.	mean	lim.	mean	lim.	mean	lim.	mean	lim.
26.5	1976	42	14	301	647	165	337	452	1490	293	810	248	248	120	120	202	202	81	81
26.5	1977	42	29	308	932	152	496	347	971	171	515	258	874	123	462	319	952	162	510
26.5	1978	37	22	—	—	—	—	384	720	197	382	—	—	—	—	211	446	79	208
26.5	1979	48	15	279	528	131	268	350	561	177	292	214	251	88	108	272	773	129	404
	All	—	—	291	662	144	344	383	936	210	500	240	458	110	230	251	593	113	301
	STIE			261	656	122	399												
26.0	1976	42	10	288	532	139	275	413	1153	216	623	248	248	120	120	202	202	81	81
26.0	1977	42	17	274	613	130	317	324	719	158	375	258	738	123	387	240	381	110	189
26.0	1978	37	3	—	—	—	—	316	383	156	192	—	—	—	—	174	174	55	55
26.0	1979	48	6	254	349	115	167	350	504	177	261	201	201	79	79	212	341	90	161
	All			265	454	123	227	351	690	177	363	236	396	107	195	207	275	84	122
	STIE			213	315	91	146												

T_{crit}—*SST* value below which production in the mixed layer becomes only light limited
obs—Number of weekly maps for which NOAA *SST* & *DML* data were used per year
% Hi—Percentage occurrence of *SST* values less than T_{crit}
P. Prod.—Estimated primary production—mg C $m^{-2}d^{-1}$
V. Flux—Estimated carbon flux—mg C $m^{-2}d^{-1}$
Mean—Average values from model
Lim.—Includes *xs* production and flux calculated from nutrient budget considerations
All—Grand means for 1976–1979 computed based on seasonal averages
STIE—Values computed for the period 24 July–5 Dec 1979

the ratio of $TPP + xs\Sigma PP_{ml}$ to TPP which, as shown in Table 3, is approximately 2.5 and to multiply the results calculated using Eqs. 4 and 5 by this factor. The second way would be to modify the model to allow events from one week to influence the next and to further permit biomass changes. The first modification to the model would not change the systematics of our calculations. The second modification would probably amplify the seasonal differences but would not significantly change our conclusions regarding the frequency or timing of high production and high particulate carbon sedimentation events. Therefore we will simply tabulate the excess production and flux and use this information summed on a seasonal basis with euphotic zone production and particulate carbon flux to provide an upper limit to these values.

3. History of primary production and particulate carbon flux at 5N, 82W from 1976–1979

Weekly averaged *SST* and *DML* data for this site were obtained by interpolation from contour maps of these variables published by NOAA/NMFS (La Jolla). Data gaps for the four week period (Aug 16–Sept 12 1979) were filled with data provided by F. Miller (NOAA/NMFS): *SST* from ships' raw observations and *DML* estimated crudely from wind data. Data for the period 1 January 1976–31 May 1979 were also obtained from the NOAA/NMFS maps but gaps were left unfilled.

Cloudiness data for the period 31 May through 12 December 1979 were taken to be the mean of weekly averaged ships' log data for the two 5° squares: 0–5N, 80–85W and 5–10N, 80–85W. For the period 1 January 1976 through 31 May 1979 monthly averaged cloudiness data from the climatological atlas of Hastenrath and Lamb (1978) were used. The monthly averages ranged from 0.48 (Feb., March) to 0.86 (August) and the mean climatological cloudiness for the second half of the year at 5N was 0.79 ± 0.04 (σ). This was slightly higher than NOAA data for the period of the STIE experiment (0.77 ± 0.03 (σ), calculated by monthly averages). The difference between these averages is insignificant and indicates no systematic bias of the NOAA cloudiness data.

Comparison of the NOAA weekly observations of cloud cover, *SST*, and *DML* with those observed during the two cruises show reasonable agreement (Fig. 5). Over the latter half of the year, the NOAA cloudiness data show relatively little variability, consistent with the fact that the STIE area is located at the mean position of the Intertropical Convergence Zone (ITCZ). The NOAA/NMFS *SST* data appear to be about 0.5°C high relative to C-FATE observations. Consequently 26.5°C rather than 26°C was chosen as the transition temperature from a nutrient-limited to light-limited mixed layer. The *DML* data agreed with the *Knorr* but not the *Gilliss* observations and is explained by a relatively sparse number of observations used in the NOAA maps near the end of the year.

NOAA data for 1976 through 1979 show that events where *SST* fell below 26.5°C appear clustered predominantly in the first and final four months of the year; coldest

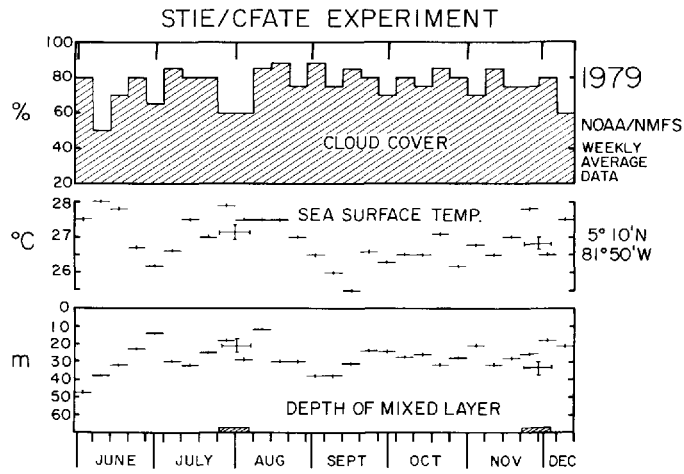

Figure 5. Weekly averages of cloudiness, sea-surface temperature (*SST*), and depth of the mixed layer (*DML*) for the period 31 May through 12 December 1979. Shaded blocks above the time axis denote the periods of the cruises; corresponding to these periods are indicated the means and standard deviations of the shipboard observations in bold lines. Mean cloudiness data agreed well for both cruises. The *SST* data appear to be systematically 0.5°C high and *DML* data agree for the *Knorr* cruise but not so well for the *Gilliss* cruise.

sea-surface temperatures were observed typically between January and March. The mixed layer depths tended to shallower values in the first half of three out of four years studied, consistent with the trends observed in the Panama Bight by Forsbergh (1969).

The mean observed *Knorr* and *Gilliss* integrated production values were 355 (9 casts) and 280 (4 casts) mg C m^{-2} d^{-1} respectively and were calculated by integrating over 6 depth intervals sampled for ^{14}C incubations. These are compared with calculated values of 286 and 174 mg C m^{-2} d^{-1} which were based on average cloudiness, *SST* and *DML* values of 0.6, 27°C and 18 m and 0.75, 27°C, and 35 m respectively for the two cruises. Particulate carbon flux estimates for the 2 cruises were 138 and 59 mg C m^{-2} d^{-1} respectively. The main difference between the calculated and observed production values is attributable to the fact that calculated production is integrated continuously as opposed to discretely in the case of the ^{14}C data. The calculated results were 396 and 191 mg C/m^2/d when integrated over bottle depths used on the two cruises. A second difference was that more days of cloudiness and *SST* data than days of ^{14}C data contributed to the averages for the 2 cruises (Fig. 1). Using NOAA/NMFS data for the two week intervals (Fig. 5) for both *Knorr* and *Gilliss* cruises yielded values of 249 and 207 mg C m^{-2} d^{-1}. Although these values were 13% low and 19% high compared with those based on ship's observations for the 2 cruises, our calculations yield systematically consistent production estimates using either shipboard or NOAA/NMFS data.

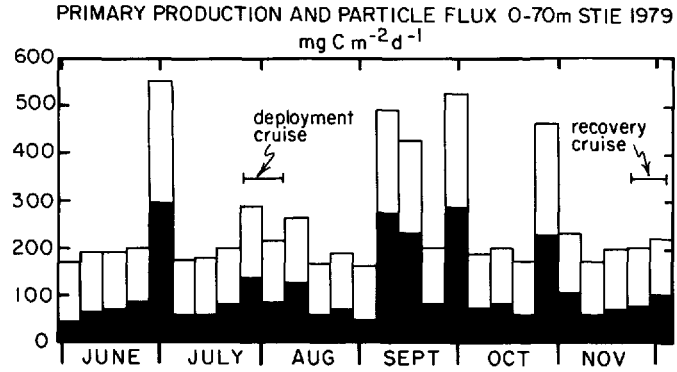

Figure 6. Calculated weekly averaged primary production (open bars) and particulate carbon flux (shaded bars) for the euphotic zone (T_{crit} = 26.5°C) during STIE. Coastal Zone Color Scanner (CZCS) images for 28 July and 30 Oct 1979 indicated surface chlorophyll levels of 0.1 and 0.4 mg m^{-3} respectively. The CZCS data are consistent with the model and lend further support to the choice of T_{crit} = 26.5°. There were possibly 4 events of high production due to nutrient enrichment in the mixed layer during the period of the experiment.

We have estimated production and carbon flux using T_{crit} = 26.5 and 26.0°C as a means of distinguishing between *possible* and *probable* events of high production and flux. Using T_{crit} = 26.5°C for the period of STIE, production averaged 261 (range 163–528) mg C m^{-2} d^{-1} and carbon flux averaged 122 (range 50–290) mg C m^{-2} d^{-1} (Fig. 6 and Table 2). Upper limits to production and particulate carbon fluxes were 660 and 340 mg C m^{-2} d^{-1} respectively (Table 3). During STIE, *possible* high production events in the mixed layer (SST < 26.5°C) occurred during the weeks beginning 28 June, 5 September, 26 September and 24 October 1979. A *probable* event (SST < 26°C) occurred during the week beginning 12 September.

Figure 7 shows production and flux estimates for the years 1976–1979 evaluated using T_{crit} = 26.5 and 26.0°C. Irrespective of assumed T_{crit} value, the patterns suggest that particle production and flux can vary substantially from year to year and seasonally. The calculations further suggest that while production can vary by a factor of ~3.5 (range 170–620 mg C m^{-2} d^{-1}), particulate carbon flux can vary by an order of magnitude (range 40–340 mg C m^{-2} d^{-1}). Since we believe that the model deamplifies seasonal differences, greater variation is likely.

4. Summary

In the STIE area solar radiation and nutrient availability are major factors controlling production in the mixed layer and below the mixed layer. Fractional cloud cover, sea-surface temperature and mixed layer depth are the three important parameters which can be used to predict euphotic zone primary production and particulate carbon flux. Evidence from Marra *et al.* (1983) suggests that variability in

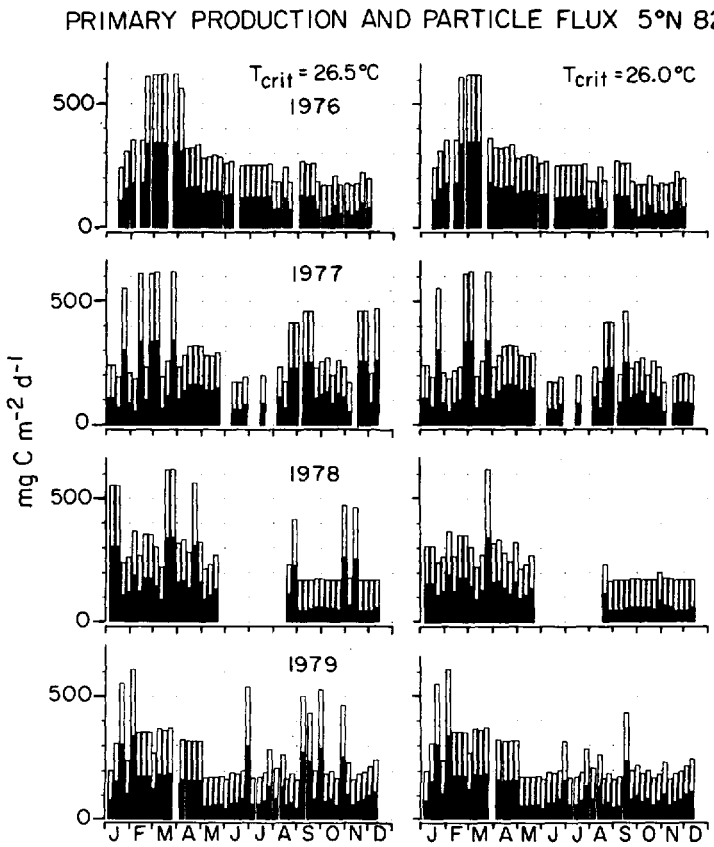

Figure 7. Calculated weekly averaged primary production and particulate carbon flux (shaded bars) for the euphotic zone for the years 1976 through 1979. Estimates are made for two values of T_{crit} = 26.5°C and 26.0°C to distinguish between *possible* and *probable* events of high production and particulate carbon flux. Weekly averaged production varies by a factor of three at the STIE site. Values fall below those typical of the Panama Bight.

phytoplankton will be expressed through rates of primary production rather than through biomass changes. According to data, production is modulated by variations in solar irradiance incident at the seasurface which is primarily due to variations in cloudiness (Fig. 1). This is consistent with the conclusions of Walsh (1976) that the event frequency, 0.1–0.2 cycles d^{-1}, is a significant factor in the variability of primary production and phytoplankton—zooplankton interactions for areas similar to the STIE site.

Primary production variations appear to be subdued on a seasonal basis compared with those observed by Forsbergh (1969) in the Panama Bight (Tables 1 and 3). January to April and May to December production in the Panama Bight appears to be roughly 95% and 25% higher, respectively, than at 5N, 82W. Over a given year, weeks

of high production and particle flux appear to occur between 10 and 30 percent of the time due to the entrainment of nutrient-enriched upper thermocline water into the mixed layer. This variability is most likely linked to upwelling activity to the north and east of the STIE area during January to April (Forsbergh, 1969). Our data suggest that the months September and October have a higher than average incidence of high production events which may be explained by entrainment of nutrients into the mixed layer during the passage of severe storms prevalent during this season.

The model shows that 1979 was a year of relatively low production in comparison to 1976 and 1977. During STIE there were possibly three week-long periods when primary production was double that of average conditions. Over a year, average weekly production may vary by a factor of three at this location.

If particulate carbon flux through the base of the euphotic zone is equal to "new" production (Eppley and Peterson, 1979) then our calculations suggest that particulate carbon flux can vary over a greater range than does total production. The impact of these variations in flux on collection rates of particulate material by deeper traps depends on additional factors such as grazing organism activities and water column dynamics. This model is only applicable to the specific location of 5N 82W in the Panama Basin. It probably could be used to describe the variations in production and particulate carbon flux within the Panama Basin with some modification.

Acknowledgments. We would like to thank the captains, crews and scientific parties of the R/V *Knorr* and R/V *Gilliss* for assistance in collecting these data and Dr. D. W. Spencer, who organized the Sediment Trap Intercomparison Experiment and was chief scientist on the *Knorr*, and Dr. S. Honjo who served as chief scientist on the *Gilliss*. Mr. Forrest Miller at NOAA/NMFS (La Jolla, CA) deserves special thanks for providing the cloudiness, *SST* and *DML* data used in the model. Drs. P. E. Biscaye and W. D. Gardner served as internal reviewers of the manuscript. Dr. I. Fung and the two anonymous reviewers are thanked for their critical comments. This research was supported under Office of Naval Research Grants N00014-75-C-0210, N00014-80-C-0098 and by The National Science Foundation grant, OCE79-09074. This is contribution number 3569 of the Lamont Doherty Geological Observatory.

REFERENCES

Bishop, J. K. B., R. W. Collier, D. R. Ketten and J. M. Edmond. 1980. The chemistry, biology and vertical flux of particulate matter from the upper 1500 m of the Panama Basin. Deep-Sea Res., *27*, 615–640.

Denman, K. L. and T. Platt. 1977. Biological prediction in the sea, *in* Modelling and Prediction of the Upper Layers of the Ocean, E.B. Kraus, ed., Pergamon Press, NY, 251–260.

Dugdale, R. C. and J. J. Goering. 1967. Uptake of new and regenerated forms of nitrogen in primary productivity. Limnol. Oceanogr., *12*, 196–206.

Dunstan, W. M. 1973. A comparison of the photosynthesis-light intensity relationship in phylogenetically different marine microalgae. J. Exp. Mar. Biol. Ecol., *13*, 181–187.

Eppley, R. W. and B. J. Peterson. 1979. Particulate organic matter flux and planktonic new production in the deep ocean. Nature, *282*, 671–680.

Eppley, R. W., E. H. Renger and W. G. Harrison. 1979. Nitrate and phytoplankton production in southern California coastal waters. Limnol. Oceanogr., *24*, 483–494.

Forsbergh, E. D. 1969. On the climatology, oceanography and fisheries of the Panama Bight. Inter-Amer. Trop. Tuna Comm. Bull., *14,* 386 pp.

Hastenrath, S. and P. J. Lamb. 1978. Climatic atlas of the tropical Atlantic and eastern Pacific Oceans. University of Wisconsin Press, Madison, Wisconsin.

Ivanoff, A. 1977. Oceanic absorption of solar energy, *in* Modelling and Prediction of the Upper Layers of the Ocean, E. B. Kraus, ed., Pergamon Press, NY, 47–71.

Jassby, A. D. and T. Platt. 1976. Mathematical formulation of the relationship between photosynthesis and light for phytoplankton. Limnol. Oceanogr., *21,* 540–547.

Johnson, J. H., G. A. Flittner and M. W. Cline. 1965. Automatic data processing program for marine synoptic radio weather reports. U.S. Fish Wldlf. Ser. Spec. Sci. Rept., Fisheries No. 503, 70 pp.

Kiefer, D. A. 1973. Chlorophyll *a* fluorescence in marine centric diatoms: responses of chloroplasts to light and nutrient stress. Mar. Biol., *23,* 39–46.

Kraus, E. B. and J. S. Turner. 1967. A one dimensional model of the seasonal thermocline. II. The general theory and its consequences. Tellus, *19,* 98–105.

Love, C., Ed. 1970–1977. Eastropac Atlases, 1–11, Circular 330, Nat. Mar. Fish. Ser., Washington D.C., U.S.A.

Marra, J., P. H. Wiebe, J. C. Stepien and J. K. B. Bishop. 1983. Primary production and plankton distribution at the site of the Sediment Trap Intercomparison Experiment (Panama Basin). J. Mar. Res., (submitted).

Platt, T., K. Denman and A. D. Jassby. 1977. Modelling the productivity of phytoplankton, *in* The Sea, Vol. 6, E. Goldberg, ed., Wiley, NY, 807–856.

Strickland, J. D. H. 1958. Solar radiation penetrating the ocean. A review of requirements, data and methods of measurement, with particular reference to photosynthetic productivity. J. Fish. Res. Board Can., *15,* 453–493.

Walsh, J. J. 1976. Herbivory as a factor in patterns of nutrient utilization in the sea. Limnol. Oceanogr., *21,* 1–13.

Yentsch, C. S. and R. W. Lee. 1966. A study of photosynthetic light reactions, and a new interpretation of sun and shade phytoplankton. J. Mar. Res., *24,* 319–337.

Received: *15 June, 1982;* revised: *18 October, 1983.*